# 4D Optical Link Tomography: First Field Demonstration of Autonomous Transponder Capable of Distance, Time, Frequency, and Polarization Resolved Monitoring

Takeo Sasai<sup>1,4</sup>, Giacomo Borraccini<sup>2</sup>, Yue-Kai Huang<sup>2</sup>, Hideki Nishizawa<sup>1</sup>, Zehao Wang<sup>3</sup>, Tingjun Chen<sup>3</sup>, Yoshiaki Sone<sup>1,4</sup>, Tatsuya Matsumura<sup>1</sup>, Masanori Nakamura<sup>1,4</sup>, Etsushi Yamazaki<sup>1,4</sup>, and Yoshiaki Kisaka<sup>1,4</sup>

<sup>1</sup>NTT Network Innovation Laboratories, NTT, 1-1 Hikari-no-oka, Yokosuka, Kanagawa, 239-0847 Japan 
<sup>2</sup>NEC Laboratories America, 4 Independence Way, Princeton, NJ 0854 USA 
<sup>3</sup>Duke University, Durham, NC, USA 
<sup>4</sup>NTT Device Innovation Center, NTT, 1-1 Hikari-no-oka, Yokosuka, Kanagawa, 239-0847 Japan 
takeo.sasai@ntt.com

**Abstract:** We report the first field demonstration of 4D link tomography using a commercial transponder, which offers distance, time, frequency, and polarization-resolved monitoring. This scheme enables autonomous transponders that identify locations of multiple QoT degradation causes. © 2024 The Author(s)

### 1. Introduction

To avoid inflexibility for network equipment selection so-called "vendor lock-in", a wide range of optical networks including data center interconnects are transforming towards openness and disaggregation [1]. While accurately characterizing the link is crucial for establishing a new optical path and conducting fault analysis, such multivendor/domain networks introduce an increased risk of the variability in network component characteristics and the inaccessibility to certain components or domains. If component-wise parameters are accurately obtained solely from network endpoints (i.e., transponders), it would allow for vendor/domain-independent and scalable telemetry, facilitating the automation of link performance analysis, provisioning, and fault localization.

The longitudinal monitoring at a coherent transponder, enthusiastically studied in recent years, can be a potential solution due to its capability of end-to-end distance-resolved monitoring solely by processing received signals [2,3]. This approach utilizes fiber nonlinearity to localize power events. By performing this function using multiple wavelengths, frequency-resolved monitoring is possible, allowing for the inspection of individual amplifiers without the need for accessing node equipment. Such a "2D link tomography" was demonstrated in [4], followed by a proposal for use in a network-wide view [5], and extension to the C+L bands [6] and polarization dimensions [7,8]. However, these demonstrations typically used high fiber launch power to excite sufficient nonlinearity, inhibiting the practical application of the tomography to commercial networks.

In this work, we demonstrate 4D optical link tomography, which visualizes optical power in distance, time, frequency, and polarization dimensions using a commercially available 800-Gbps transponder. This scheme allows commercial transponders to autonomously identify the location of multiple QoT degradation causes as an auxiliary function, including time-varying power anomalies (e.g., bending loss), spectral anomalies, and excessive PDL. We also show that, by averaging power profiles over available dimensions, the power profile SNR is enhanced enough to locate multiple field lumped losses, enabling the tomography to operate at lower power than system optimal levels.

## 2. 4D Optical Link Tomography and Experimental Setup

Fig. 1(a) shows the experimental setup. The link under test comprises of 53.4 km, 54.8 km, and 54.8 km spans of field deployed fibers around the Duke University. The sensing channel for the tomography is an 800-Gbps 130-GBd-class signal from a commercially available transponder, employing a dual-polarization (DP) PCS-64QAM format. 4 × 400Gbps (DP uniform 16QAM 64GBd-class signals) data channels are co-propagated with their frequencies set to 192.025, 193.025, 194.025, and 195.045 THz and multiplexed by an arrayed-waveguide grating (AWG). We emulate a 100-GHz-spaced 39-ch full C-band dense wavelength division multiplexing (DWDM) transmission by loading amplified spontaneous emission (ASE) noise shaped by a wavelength selective switch (WSS). The signals are then multiplexed by the WSS. Fig. 1(b) shows the transmitted spectrum after the first booster erbium-doped fiber amplifier (EDFA). Throughout this experiment, we ensured that the power level of the sensing signals matched that of as adjacent channels. The field fibers have an average chromatic dispersion (CD) of 17.55 ps/nm/km. To demonstrate the localization of a time-varying bending loss and an excessive PDL, we inserted a variable optical attenuator (VOA) at the beginning of the second span and a 3-dB PDL emulator at the beginning of third span.

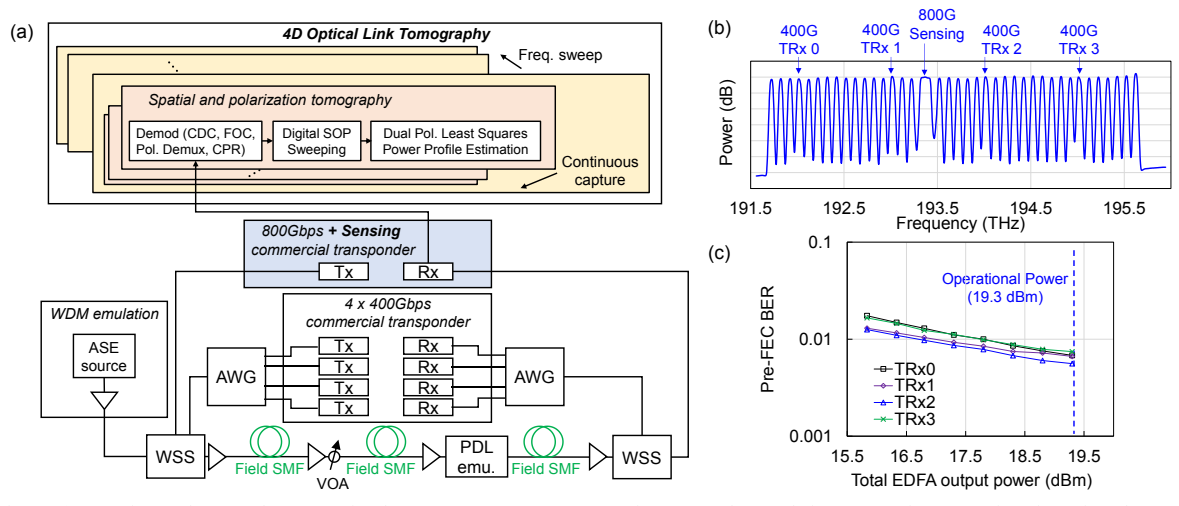


Fig. 1 (a) Experimental setup. (b) Transmitted spectra. (c) Pre-FEC BER of  $4 \times 400$  Gbps real-time transceivers as a function of total EDFA output power (3-span average). Operational power is fixed to 19.3 dBm.

For 400Gbps channels, pre- and post-FEC BER was measured by the real-time transponder. Fig. 1(c) shows the pre-FEC BER measured by four transceivers as a function of the total EDFA output power (uniformly set for all three spans with constant output power mode.) We also observed that the corresponding post-FEC BER were error-free. Based on these observations, we set the launch power to 19.3 dBm, where the pre-FEC BERs still do not reach its optimal peak, confirming the system is working in a more linear regime. This operation is due to the limited maximum output power of the EDFAs.

For the sensing signal, we captured the raw waveforms received by the 800 Gbps transponder at intervals of 0.55 seconds. To obtain the 4D tomography results, we initially estimated the polarization-wise power profiles using least squares-based algorithm [8]. After the demodulation process including CD compensation (CDC), frequency offset compensation (FOC), polarization demultiplexing, and carrier rhase recovery (CPR), we swept the state of polarization (SOP) of both the demodulated and reference signals used for the least squares. This adjustment was performed to search for the principal axis of the targeted PDL [8]. Time-resolved monitoring is enabled by iterating the procedure for continuously captured waveforms. To perform the tomography in the frequency dimension, we varied the center frequency of the sensing channel.

## 3. Experimental Results

Fig. 2 shows the 4D link tomography results. From the spatial and spectral tomography shown in Fig. 2(a), we can observe locations of EDFA as well as some orthogonal traces due to spectral tilts. Fig. 2 (b) is the spectral tomography picked up from the input of the first and third spans. At the first span input (blue), we observe a spectral tilt that decreases towards the lower frequency direction, with a 2-dB power difference observed at the spectral edges. On the other hand, the spectral tomography at the third span input (red) shows a tilt emphasized in the opposite direction. Moreover, we observe from the tomography a significant drop in the spectrum around 195.325 THz. This observation is correlated with OSNR values (green) monitored by  $4 \times 400$ -Gbps transceivers, with TRx 3 at 195.025 THz showing more OSNR degradation. This implies that the tomography can locate the root cause of the QoT degradation observed at transceivers. The spectral tomography and the OSA references show agreement, with a maximum error of 0.62 dB and an RMS error of 0.29 dB. Fig. 2(c) shows the polarization tomography results at 193.4 THz. While the powers of two orthogonal polarizations in the first and second spans remain consistent, discrepancy are observed from the beginning of the third span, corresponding to the insertion point of the PDL emulator. Fig. 2 (d) shows the temporal tomography at locations 2.0 km, 55.0 km, and 109.0 km. The sensing signal frequency is set to 193.4 THz. The observed power variation at 55.0 km (purple) follows the monitored value of the VOA inserted at the beginning of the second span. The constant optical power observed at 2.0 km and 109.0 km results from the constant output power mode operation of EDFAs.

Finally, we show the spatial tomography enhanced by averaging over time (100 waveforms), polarization (two), and frequency (15 frequencies) dimensions (Fig. 3(a)). A non-uniform power at the third span input is due to the insertion loss of PDL emulator. Fig. 3(b) and (c) are the anomaly indication by subtracting fiber loss slopes from Fig. 3(a) for the second and third span, respectively. The tomography reveals large lumped losses in the field fibers and

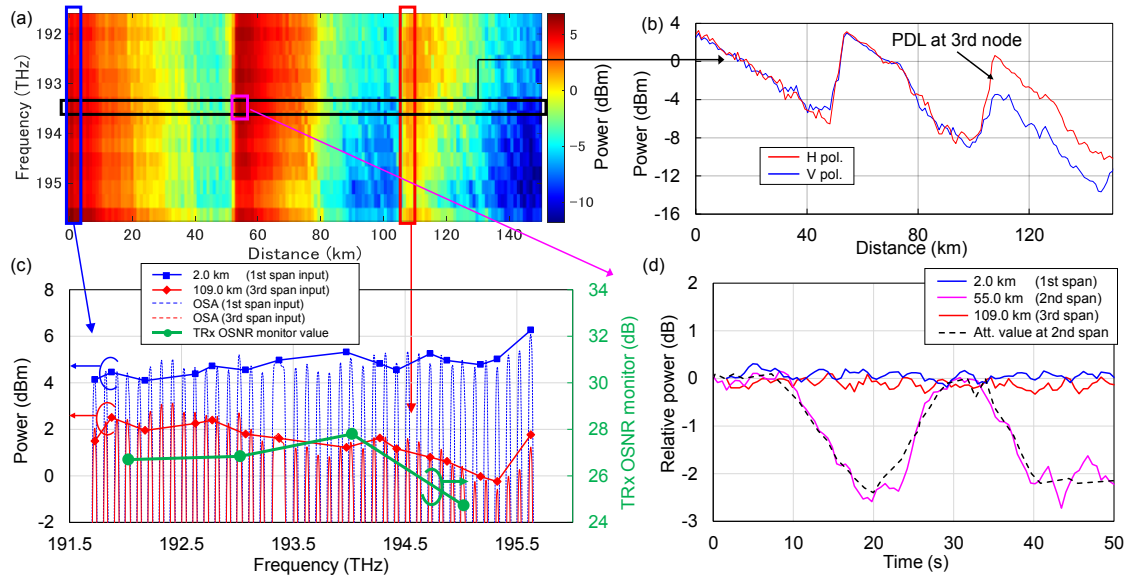


Fig. 2. 4D link tomography results. (a) Waterfall plot of spectral and spatial tomography. (b) Polarization and spatial tomography results. (c) Spectral tomography at first and third span input. OSNR monitored by  $4 \times 400 \text{Gbps}$  TRx are also shown. (d) Temporal tomography at the span inputs.

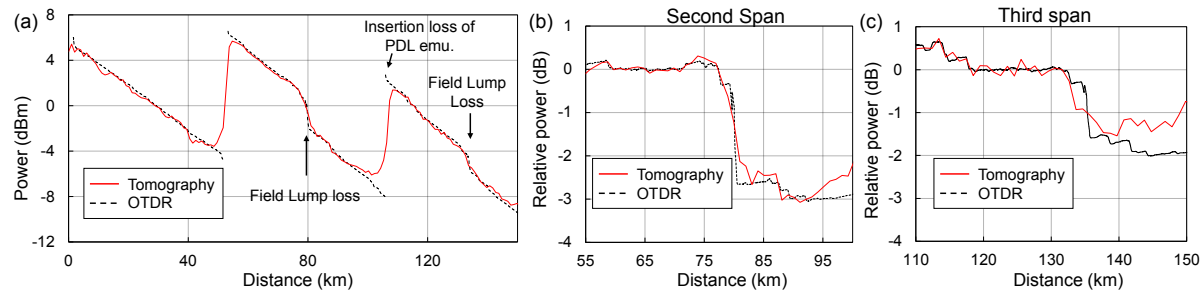


Fig. 3 (a) Spatial tomography results averaged over time, polarization, and frequency dimensions. (b)(c) Closeup of power profiles around field lumped losses in second and third spans, respectively. Fiber loss slopes are subtracted.

also appears responsive to other minor events distributed along the spans. Despite the more severe conditions under lower power operation in the third span (Fig. 3(c)), the presence of a 1.5 dB lumped loss is clearly observed.

#### 4. Conclusion

We have reported the first field trial of 4D optical link tomography using commercially available transponders. This scheme visualizes spatiotemporal, spectral, and polarization-wise power profile, successfully localizing the multiple QoT degradation cause, including a time-varying loss, spectral tilts and drop, and PDL. Furthermore, the power profile SNR is enhanced by averaging over all dimensions available, enough to locate field lumped losses even in the low nonlinearity regime where the launch power was operated at less than system's optimal levels.

## Acknowledgement

This work was supported in part by NSF grants CNS-2211944 and CNS-2330333. We thank the Duke Office of Information Technology (OIT) team and the members of NTT DevIces America Inc. for their support.

### References

- [1] M. Newland et al., "Open optical communication systems at a hyperscale operator," JOCN, 12, C50-C57 (2020).
- [2] T. Tanimura et al., "Experimental demonstration of a coherent receiver that visualizes longitudinal signal power...," ECOC, PD.3.4, 2019.
- [3] T. Sasai et al., "Digital longitudinal monitoring of optical fiber communication link," JLT, 40(8), 2022.
- [4] T. Sasai, et al., "Revealing Raman-amplified power profile and Raman gain spectra with digital backpropagation," OFC, M3I.5, 2021.
- [5] T. Tanimura et al, "Concept and implementation study of advanced DSP-based fiber-longitudinal...," JOCN, 13(10), E132-E141, 2020.
- [6] M. Sena et al., "Advanced dsp-based monitoring for spatially resolved and wavelength-dependent amplifier...," JLT, 41(3), 989-998, 2022.
- [7] M. Eto, et al. "Location-resolved PDL monitoring with Rx-side digital signal processing in multi-span..." OFC, Th1C.2, 2022.
- [8] M. Takahashi, "Experimental demonstration of monitoring PDL value and location using DSP-based longitudinal..." ECOC, P14, 2023.